applied sciences

MDPI

Article

Revisiting Cracking in Reinforced Concrete Beams: An Updated Analysis

Adelino V. Lopes [1] and Sergio M. R. Lopes [2,*]

[1] INESC Coimbra, Department of Civil Engineering, University of Coimbra, 3030-788 Coimbra, Portugal
[2] Centre for Mechanical Engineering, Materials and Processes, Department of Civil Engineering, University of Coimbra, 3030-788 Coimbra, Portugal
* Correspondence: sergio@dec.uc.pt

Featured Application: The study's findings have implications for the design of reinforced concrete structures, as they reveal new insights into the location and prediction of cracks in beams subjected to bending. Based on these findings, the authors recommend that design rules for predicting crack widths should be updated to incorporate the sag-to-free-span ratio as a key factor.

Abstract: As materials and structural optimization continue to be important in design, structural safety checks for service limit states have become increasingly important. One key aspect of these checks is the controlling of cracks to prevent them from affecting the structure's function or appearance. However, the authors have found that current regulations do not accurately reflect the reality of crack behavior. This is the case of the crack spacing. To address this issue, the authors conducted experiments on 27 reinforced concrete beams to investigate crack location, cracking moment, corresponding deflection, and crack width values as sag increases. Their main finding was that cracks tend to appear at the stirrup locations, and that crack width increases linearly with the sag-to-free-span ratio up to the yielding point. They also concluded that increasing the amount of tensile reinforcement is an effective way to reduce crack width for the same sag.

Keywords: cracking; RC beams; Crack position; crack spacing; crack width; Moment of cracking; cracking deflection; experimental work

Citation: Lopes, A.V.; Lopes, S.M.R. Revisiting Cracking in Reinforced Concrete Beams: An Updated Analysis. *Appl. Sci.* **2023**, *13*, 3926. https://doi.org/10.3390/app13063926

Academic Editor: Laurent Daudeville

Received: 5 March 2023
Revised: 14 March 2023
Accepted: 16 March 2023
Published: 20 March 2023

1. Introduction

The constant optimization of the use of materials in structures has made these materials more requested, which is why Service Limit States (SLS) gain relevance in terms of safety checks. Deformation and cracking are phenomena inherent to reinforced concrete elements when subjected to imposed loads or deformations [1]. As the American Concrete Institute (ACI) [2] states, reinforced concrete members subjected to flexure shall be designed to have adequate stiffness to limit deflections or any deformations that adversely affect strength or serviceability of a structure.

The regulatory verification [1,2] of deflection can be carried out indirectly by geometrically imposing the height of beams and slabs, or it can be carried out by comparing a design value with a limit value. The question is the evaluation of the design value. In general, the uncracked structure (i.e., admitting elastic behavior) is considered subject to a certain load (depending on the permanent loads and the variable action). In the case of Eurocode 2 (EC2) [1], the long-term effects of creep are taken into account by changing the modulus of elasticity and the long-term effects of shrinkage by consideration of an additional curvature. In the case of ACI [2], these two types of long-term effects can be considered by multiplying the deformation by a coefficient. But the basic question remains: how to evaluate the instantaneous deflection? It is not intended to know here how this deflection can be evaluated if a substantial part of the structure is cracked, but it is intended to know when cracking begins.

In fact, to calculate the deflection, for example, EC2 [1] proposes an interpolation between the elastic deflection and the deflection in a fully cracked structure. Among other parameters, this interpolation depends on the cracking moment of the section.

Cracking, in particular, is caused by different factors, conditioning both the stiffness and durability of structures. Cracking is normal in reinforced concrete structures subject to bending, shear, torsion, or tension resulting from either direct loading or restraint or imposed deformations. Cracks may also arise from other causes such as plastic shrinkage or expansive chemical reactions within the hardened concrete [1]. Such cracks may be unacceptably large, but this issue is outside the scope of this work. Anyway, cracking reduces stiffness of RC members, and increases deformation when loads act on the structure.

The study of cracking, particularly crack width and spacing, has been a topic of investigation for long time. In 1943, Watstein [3] conducted one of the earliest works on the subject, where he tested axially reinforced cylinders by applying tensile forces to the reinforcement and observing the resulting deformations of the concrete, including crack width and spacing. Even then, Watstein concluded that crack width is proportional to tension in the reinforcement after cracking begins. Additionally, he suggested that new cracks will not appear if the tensile strength of the concrete is not exceeded, although he did not explicitly state this.

However, several works [4,5] involving deep beams appeared. These tests involved supposedly bending beams: in fact, the arching effect was not negligible, with slenderness ratios of L/h = 5.7 and L/h = 6.2. As a result, the shear effects on the web of the beams were significant, and this caused cracking that was different from the cracking observed in normal beams subject to bending. These works exhibited a relevant characteristic in the methodologies used to control cracking, which are similar to those currently employed in regulations [6]. In particular, the evaluation of crack width was heavily dependent on the steel stress, whereas the bond between steel and concrete, cover, and reinforcement ratio were primarily considered in the assessment of crack spacing.

A little later (1983), Bazant et al. [7] used a theoretical formulation (using the energy criterion of fracture mechanics as well as the strength criterion) to estimate crack width and spacing in RC elements under pure tension. The proposed theoretical formulation was confirmed by experimental results obtained by other authors. It should be emphasized that the real unknown in the study was the crack spacing, which was found to be a function of several factors, including the axial strain of the bars, bar spacing, bar diameter, fracture energy of concrete, and its elastic modulus. Since then, it became reasonably well-known how to calculate the width once the crack spacing is determined. The crack width calculation used in this study was similar to the expression used in European Concrete Design Standard EC2 [1]. The adaptation for beams subject to bending consisted of determining an area around the tensile reinforcement where the stress field would be assumed to be uniform. The results then determined were, however, updated, namely, the deformation for the onset of cracking and the minimum spacing between cracks. The study did not consider the presence of stirrups in the RC beams.

In 1988, Leonhardt [8] presented a work primarily applicable to large structures; however, the general concepts presented are applicable to any concrete structure. Leonhardt explicitly wrote that “Cracking occurs when tensile stresses exceed the tensile strength of concrete. Therefore, to control concrete cracking, the tensile strength of concrete is of primary importance”. However (differently), he also wrote that “concrete cracks when the tensile strain exceeds 0.010 to 0.012%. This limiting tensile strain is essentially independent of concrete strength”. Another aspect that deserves to be mentioned in the context of the present work is that Leonhardt proposed that “The 5 percentile of the tensile strength should be used in design to locate areas in the structure that are likely to crack”. Leonhardt recommended using small bar diameters and a small spacing of reinforcement for the best control of cracking. He also drew attention to the minimum tensile reinforcement for preventing sudden failure when cracking occurs.

Around the 1990s, experimental works that incorporated computational methodologies began to emerge, with Braam's PhD thesis [9] being one example. Having focused his study on T-deep beams, Braam completely ignored the presence of stirrups in the location of the cracks. All the theory so far developed from RC elements subject to pure tension continued to be followed and applied to beams subject to bending.

By this time (1990s), the methodologies for estimating crack spacing and width had become well-established. First, the crack spacing was estimated and then the width. Some models had previously considered the crack width to be dependent on the diameter of tensioned reinforcement but were quickly abandoned [7,10]. The crack width was considered proportional to steel stress and crack spacing. This model persists in the current regulations.

There is also a transformation of the models to evaluate crack widths and the spacing. Initially, the strategy for establishing these models involved selecting several parameters with an impact on cracking and determining their coefficients using statistical regressions. After that, the strategy shifted towards using semi-theoretical and semi-empirical formulas based on the analysis of the cracking mechanism, such as the fracture energy criterion and strength criterion. These formulas are derived from mechanical models, but some of the coefficients are determined through experiments. The current models used in main regulations have used this approach [1,2].

Considering the crack spacing, by this time (the 1990s), many parameters were considered: the concrete cover c [8,9,11–13], and/or the bar spacing [8,9,11–13], and/or the steel stress σs [11], and/or the concrete properties (compressive strength f_c, tensile strength f_{ct}, elastic modulus E_c) [7,14,15], and/or the bond stress σ_b [7,14,15], and/or the bond properties (if high bond bars or plain surface) [8], and/or the bar diameter ϕ [7–9,11,12,14], and/or the effective reinforcement ratio ρ_{eff} (determined in an effective area of concrete in tension surrounding the reinforcement) [7–9,14,15], and/or coefficient which takes account of the distribution of strain (if bending or pure tension) [8]. In general, all models were derived from knowledge of RC elements subject to pure tension. Afterwards, they were adapted to beams in bending. All ignored the possible presence of transverse reinforcement in beams.

In general, the crack spacing started to be determined from a sum of 2 terms: one directly proportional to the cover; the other directly proportional to the ϕ/ρ_{eff} ratio [16].

An interesting particularity is that, by observing the photos of beams tested by various authors [15,17,18], and taking into account the number of cracks and the spacing of the stirrups, most likely, the location of the cracks coincided with the position of the stirrups, although it is not possible to fully confirm this conclusion. On the other hand, Umberto De Maio [19], using computational analysis, determined cracks positioned between stirrups.

In Piyasena's PhD thesis [11], the issue of the effects of the presence of stirrups on RC elements under (variable) bending was addressed. Piayasena wrote: "Occurrence of flexural cracks at constant spacings in varying moment regions, . . . , has been observed by many investigators". In this regard, he cites Makhlouf [20] and Fantilli [21]. Piayasena completed, "This fact is often correlated to the spacing of stirrups, assuming that the presence of a stirrup makes the section 'weak'." In Piyasena's work, resorting to a figure where he geometrically shows the "Progressive development of primary cracks in a varying moment region", he justifies: "the stress distributions shown in figure clearly indicates that the primary crack spacing in a varying moment region is constant even if the strength along the member is unchanged."

In turn, in Makhlouf's [20] work, it is written: (i) "Visual inspection of the specimens has shown that flexural cracks are greatly affected by the location of the stirrups and are forming in their vicinities"; (ii) "Clearly, the crack spacing can be directly correlated to the spacing of the stirrups used in the specimens". These are the only sentences that the authors found in the bibliography that relate the positioning of the cracks with the placement of the stirrups. However, Makhlouf was not assertive enough, because he writes (only) in the

conclusions of the work: "Results of Groups A and B indicate that spacing of the cracks is most probably governed by stirrup spacing".

Regarding Fantelli's work [21], the authors only found a reference to stirrups, when Fantelli writes: "However, the presence of stirrups or the load history may alter the theoretical regular evolution of the cracks." However, despite the fact that, in this work, a regular spacing between cracks was verified, this fact could not have been caused by the stirrups because, purely and simply, they did not exist.

Another important issue in cracking, namely, in the evaluation of the crack width is the crack width variation along the concrete cover depth. In this work, only the crack widths on the outer surface of the RC beams were measured. In this regard, Naotunna [22], based on experimental work on RC elements subjected to pure tension, indicates that the crack width at the reinforcement is typically smaller than the crack width at the external concrete surface. This observation is similar to the findings in the previously mentioned experiments reported by other authors. This reduction depends on the reinforcement cover and the type of steel, whether smooth (plain surface) or with a rough surface (ribbed). In the case of steels with rough surfaces (high bond bars or ribbed) and with cover greater than 30 mm, the crack width on the surface of the steel can be only ~25% of the crack width on the external surface of the concrete. In the case of steels with a smooth surface, the reduction is not significant, or it may not even happen. Naotunna adds two important sayings. The first: "The crack width at the reinforcement is independent of the concrete cover depth". Second: "When primary cracks are developing, the tensile strain in reinforcement exceeds the ultimate tensile strain of the surrounding concrete. This strain difference between the steel and concrete is referred to as 'strain incompatibility'. Due to the good bond between the ribbed reinforcement and surrounding concrete, this strain incompatibility has been accumulated in the internal cracks."

As the study of cracking became preponderant, several calculation models were developed, namely, in terms of evaluating crack width that are important to control. However, as for crack spacing, it has not yet been possible to generate a consensus at this level, given the different criteria developed, namely, when confronted with reality. With the present work, the authors intend to re-analyze this theme from the perspective of some specific parameters (explained below) in normal RC beams. It should be noted that it is not the objective of this work to consider the presence of any type of fiber included in the concrete.

For example, what will be the effect of positioning the transverse reinforcement in terms of crack spacing? This is another important question. In the overwhelming majority of works, it is written "cracking happens when the concrete stress equal to the tensile strength of concrete". Will it be this or "cracking happens when the strain of concrete equal to the strain strength of tensioned concrete"? That is, is cracking related to stress or strain in the concrete? As it will be seen later, in reinforced concrete elements subject to bending, cracking depends also on steel strain.

In fact, it is possible to state: deflection and cracking are two interdependent phenomena which essentially depend on the structural deformation caused by external actions over the structure. It is true that, in the mechanics of materials, a certain "strain" always corresponds to a "stress".

At the end of this point, the authors would like to draw attention to the originality of this work, reflected in the discussion and conclusion points. In these paragraphs, some with different conclusions, only the issue of increasing the cracking moment of RC sections in relation to the tensile reinforcement ratio is known [23]. From the remaining conclusions, either the authors are unaware of its publication, or are aware of numerous publications that contradict it.

2. Initial Considerations

2.1. Crack Initiation

The main codes of practice are unanimous in establishing that the strength of concrete in tension is important in cracking considerations, i.e., when ultimate stress of concrete in tension is reached, cracking starts. Furthermore, they all evaluate crack width as a function of steel strain.

For example, about the bending of RC beams, ACI [2] advocates that flexural and flexure-shear cracking is initiated by flexural cracking. When flexural cracking occurs, the shear stresses in the concrete above the crack are increased. The flexure-shear crack develops when the combined shear and tensile stress exceeds the tensile strength of the concrete. Web-shear cracking begins from an interior point in a member when the principal tensile stresses exceed the tensile strength of the concrete.

Thus, it is common to make the beginning of cracking correspond to a certain load (cracking load P_{cr}) which determines the boundary between the known State I and State II of the behavior of RC structures. State I corresponds to the non-cracked phase, in which the behavior of the beam is essentially ensured by the concrete. Associated with P_{cr} is the respective cracking moment M_{cr}.

Considering a rectangular cross section of a RC beam, of width b, height h, whose tensile strength is f_{ct}, the cracking moment M_{cr} is determined by [24–26]:

$$M_{cr} = f_{ct} \frac{b.h^2}{6} \quad (1)$$

For the value of f_{ct}: (i) although not explicitly indicating it, the value $1.25 f_{ctm}$ is assumed by ACI [2]; (ii) the EC2 Handbook [24] indicates the mean value of axial tensile strength of concrete f_{ctm}; (iii) the CEB manual [25] indicates the characteristic 5% value of axial tensile strength of concrete $f_{ctk0.05} = 0.7 f_{ctm}$; and (iv) the Structural Concrete [26] indicates the mean flexural tensile strength of concrete $f_{ctm,fl} \geq f_{ctm}$. These are substantially different values. For the purposes of this work, the mean flexural tensile strength of reinforced concrete members $f_{ctm,fl}$ was adopted as the value for f_{ct}, defined by EC2 [1]:

$$f_{ctm,fl} = max\{(1.6 - h/1000).f_{ctm}; f_{ctm}\} \quad (2)$$

where h is the total member depth (in mm).

Alternatively, consider the stress–strain diagram of concrete tensile behavior shown in Figure 1. This diagram is qualitatively equivalent to that shown in Volume 1 of MC2010 [27] in a schematic representation of the stress–strain and stress–crack width relation for uniaxial tension (according to fib Bulletin 42). Here, it is important to define the beginning of cracking. Does cracking start at point A? Or at point B? Or at some intermediate point of the line AB? Considering what is defined in Equation (1), cracking starts at point B. However, if many other contexts are considered (micro-cracks for example), cracking should start at point A. The MC2010 [27] indicates that, at tensile stresses of about 90% of the tensile strength f_{ct} (point A), micro-cracking starts to reduce the stiffness in a small failure zone. For what follows, this is not important. It is necessary to focus the attention on the strains.

Regarding the strains, MC2010 [27] indicates that the stiffness of the line OA is defined by modulus of elasticity E_{ci} (at concrete age of 28 days). Therefore, by establishing the k1 coefficient and the f_{ct} value, the ε_{ct1} strain is defined. Then, it is important to define the strain value at the point of maximum tensile strength ε_{ctu}. MC2010 [27] defines $\varepsilon_{ctu} = 0.15‰$. Leonhardt [8] proposes a value in the range {0.1–0.12‰}. In this context, note that Lima [6], in 1973, indicated values 2 to 3 times higher. For concrete that is at least 28 days old, either the value of f_{ct} (tensile strength) or the value of E_{ci} (modulus of elasticity) can be estimated from the mean value of concrete cylinder compressive strength f_{cm}. It should also be noted that the modulus of elasticity of concrete largely depend on its composition (especially the aggregates).

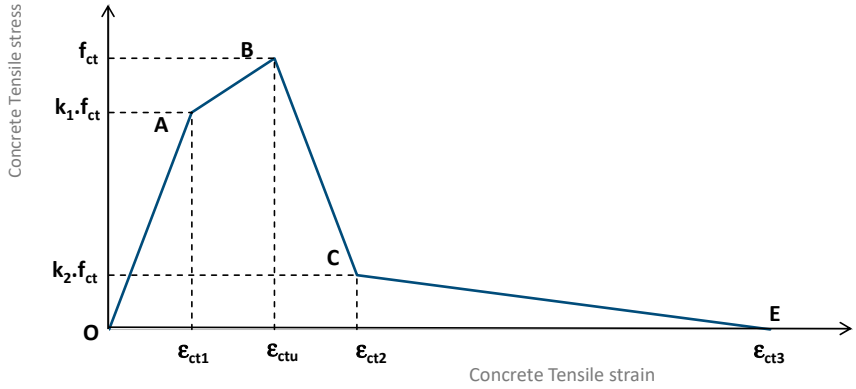

Figure 1. Stress–strain behavior of concrete in tension.

It remains to be noted that the descending part of the behavior curve shown In Figure 1, namely, the definition of points C and E, depend on the fracture energy of concrete and on the stiffening effect phenomena. For this purpose, it is known that, for concrete in tension, the crack propagation can be different for various types of concrete due to the difference in the internal structure. For normal concrete, the crack propagates in the cement paste and in the interface around the aggregates. However, for high strength concrete and concrete with lightweight aggregates, the crack propagates in the cement paste and through the aggregates due to the relatively higher strength of the cement paste.

Therefore, it can be assumed that the first crack occurs in the zone where the maximum admissible concrete strain (ε_{ct1} or ε_{ctu}) is reached. Assuming increasing loads, the resistance to tensile strength previously ensured by the concrete is transferred to the reinforcement. Loads greater than this occur in the so-called State II, where cracking develops.

2.2. Crack Control

It should be ensured that cracks will not impair the serviceability and durability of the structure or cause its appearance to be unacceptable. For EC2 [1], these specific requirements may be met by an appropriate limitation of crack widths w_{max}. If crack control is required, it should be $w_k \leq w_{max}$, where w_k is the calculated crack width (characteristic value).

ACI [2] prescribes rules for distribution of flexural reinforcement to control flexural cracking in beams. Several bars at moderate spacing are much more effective in controlling cracking than one or two larger bars of equivalent area. According to ACI [2], extensive laboratory work involving deformed bars has confirmed that crack width at service loads is proportional to steel stress. The significant variables reflecting steel detailing were found to be the thickness of concrete cover, the spacing of reinforcement, and the minimum reinforcement. Crack width is inherently subject to wide scatter even in careful laboratory work and is influenced by shrinkage and other time-dependent effects. Improved crack control is obtained when the steel reinforcement is well distributed over the zone of maximum concrete tension and crack width can be limited by an increase in the amount of reinforcement used (by reducing the stress at the service load level). When high strength reinforcing steels are used at high service load stresses, visible cracks should be expected. However, at the same time, ACI admits that crack widths in structures are highly variable. In addition, ACI establishes requirements regarding transverse reinforcement, both in terms of quantity and in terms of maximum spacing. Regarding the spacing between transverse reinforcements, ACI prescribes: Spacing of shear reinforcement placed perpendicular to axis of member shall not exceed d/2 (d means effective depth of a cross-section; d~0.9 h) in no prestressed members and indicates that shear reinforcement restrains the growth of inclined cracking.

With regard to the indirect control of crack width by limiting steel spacing, it is important to say that EC2 [1] is a little more restrictive than ACI [2]: for example, for a case

where the service stress in the steel is σy ~ 250 MPa, the limit spacing in EC2 is less than 250 mm; for ACI, this limit oscillates between {~300–~350 mm}, depending on the cover.

When calculating crack width w_k in concrete structures, EC2 standards suggest that it may be determined using the following equation:

$$w_k = S_{r,max}.(\varepsilon_{sm} - \varepsilon_{cm}) \quad (3)$$

where $S_{r,max}$ is the maximum crack spacing, ε_{sm} is the mean strain in the reinforcement under the relevant combination of loads, and ε_{cm} is the mean strain in the concrete between cracks.

Because the concrete strain ε_{cm} is significantly less than the steel strain ε_{sm}, EC2 calculates w_k based on the steel strain. The issue that needs to be highlighted here concerns the calculation of $S_{r,max}$. For EC2, $S_{r,max}$ depends on the cover of longitudinal reinforcement c, on the bar diameter ε and on the effective reinforcement ratio for longitudinal reinforcement $\rho_{p,eff}$ (defined in the effective area of concrete in tension surrounding the reinforcement). It is not important here to indicate the corresponding expressions. It is interesting to point out that, for current cases of beams, it is possible to evaluate values greater than 250 mm for $S_{r,max}$.

Regarding the maximum crack spacing, Ghali [28] proposes a (simpler) expression dependent on the cover, diameter, and average spacing of the bars. For tensile reinforcement ϕ = 12 mm, cover of c ~ 25 mm, and spacing s ~ 150 mm apart, the proposed expression determines maximum spacing between cracks $S_{r,max}$ ~ 200 mm.

To finish this point, refer to the work of Bouhjiti [29]. In this numerical work, a sufficiently succinct bibliographical review is presented on the theme "crack spacing". Confronting the experimental results of several beams, it presents a conclusion to be highlighted: there is a "Linear correlation between the mean spacing and the ratio ϕ/ρ regardless of the concrete properties". For example, if for diameters ϕ = 20 mm, it shows spacings of about ~130 mm apart; for diameters ϕ = 10 mm, the spacing can be greater than ~220 mm. Once again, the possibility of the presence of stirrups influencing the results was completely ignored.

3. Experimental Procedure

For this work, some results collected in several experimental works on beams, all carried out by the authors, were selected.

3.1. Test Procedure

All beams were subjected to a 4-point bending test, as shown in Figure 2. In the beam tests, L_1 = 950 mm and L_2 = 900 mm (constant bending zone) were measured in normal beams and L_1 = 475 mm and L_2 = 450 mm in reduced dimensions beams. In general, the tests were performed with strain control over about 120 min. In general, until shortly after the steel yielding, the deformation rate was reduced, increasing significantly (~2*) after that.

3.2. Beams

Regarding the beams, the authors tried to select the most diverse parameters: normal and reduced dimensions, different curing ages, ER (cold worked steel) and NR (hot rolled steel) ribbed steels, different (geometric) reinforcement ratios, different spacing of transverse reinforcement, and different cover. For the selected reinforced concrete beams, Table 1 specifies the geometric characteristics (L indicates the length of the beam; b the width of the rectangular cross section; h the corresponding height), the day of the test T and the value (average) expected compressive strength of concrete f_c. For beams tested in the short-term (less than 60 days of curing), the f_c value is determined by a logarithmic curve (Neville methodology [30]), which, in turn, results from a huge set of tests on different cubes of concrete with a 150 mm edge, carried out on different days. In general, more than 20 cubes, tested in groups of 3, were tested in a longer time interval. For long-term beams,

the methodology indicated in EC2 [1] (exponential curve) was used, which included cover of 20 mm for normal beams and 10 mm for Group VIII of beams.

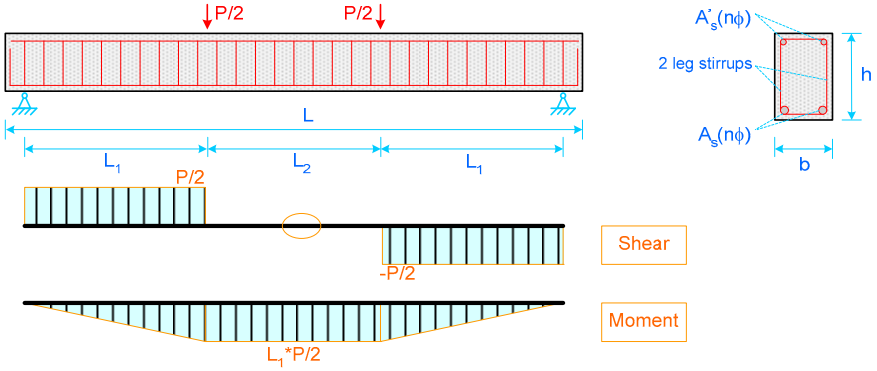

Figure 2. Test set-up.

Table 1. Description of RC beams.

Group	Beam	L (mm)	b//h (mm)	T (Days)	f_c (MPa)
I	B01.ER.2f8.2f10.f6@180	3000	205//310	33	24.4
	B02.NR.2f8.2f10.f6@180	3000	205//310	33	24.4
II	B03.ER.2f10.2f10.f6@180	3000	205//310	32	24.3
	B04.NR.2f10.2f10.f6@180	3000	200//305	32	24.3
III	B05.ER.6f12.2f10	3000	210//305	31	24.3
	B06.NR.6f12.2f10	3000	203//297	31	24.3
	B07.ER.6f12.2f10.f6@60	3000	192//305	28	24.0
	B08.NR.6f12.2f10.f6@60	3000	200//305	27	23.9
	B09.ER.6f12.2f10.f6@180	3000	200//275	26	23.8
	B10.NR.6f12.2f10.f6@180	3000	200//305	26	23.8
IV	B11.NR.3f16.2f10AR0	3000	202//301	379	33.9
	B12.NR.3f16.2f10.f6@60AR0	3000	204//302	379	33.9
	B13.NR.3f12.2f6.f6@60AR0	3000	204//302	382	33.9
	B14.NR.3f16.3f16.f6@180AR0	3000	205//305	382	33.9
V	B15.NR.3f12.2f8.f6@60AR0	3000	207//303	42	29.3
	B16.NR.3f12.2f8.f6@60	3000	202//302	41	29.2
	B17.NR.3f12.2f8.f6@60AR0	3000	207//303	40	29.0
	B18.NR.3f12.2f8.f6@180	3000	200//303	41	29.2
VI	B19.NR.3f16.2f10.f6@180AR50	3000	201//299	761	34.4
	B20.NR.3f16.2f16.f6@180AR50	3000	201//299	762	34.4
VII	B21.NR.3f12.2f8.f6@180	3000	202//307	54	36.6
	B22.NR.3f12.2f8.f6@60	3000	200//306	54	36.6
	B23.NR.3f12.2f8.f6@60AR0	3000	202//303	50	36.1
VIII	B24.ER.2f6.2f6.f4@70	1500	98.1//152	34	41.6
	B25.ER.3f6.2f6.f4@70	1500	100//153	34	41.6
	B26.ER.4f6.2f6.f4@70	1500	100//154	36	41.8
	B27.NR.3f8.2f6.f4@70	1500	101//153	37	42.0

Table 2 shows the reinforcement amounts of the selected beams: the type of steel in the "steel" column, the amount of tensile reinforcement A_s, the corresponding reinforcement ratio ρ, the amount of compressive reinforcement A'_s, the corresponding reinforcement ratio ρ', and the transverse reinforcement in the lateral and central zones, A_{sw1} and A_{sw2}, respectively. Note that the load scheme adopted, with 4 points, determines two lateral zones and a central zone in the span of the beam (see Figure 2). For example: A_s = "2f10" means 2 longitudinal bars with a diameter of 10 mm located in tensile reinforcement; A_{sw} = "f6@180" means vertical stirrups with 2 legs spacing 180 mm apart along the axis of the beam; and "AR50" means axial restraint with an initial axial force of ~50 kN.

Table 2. Reinforcement steel of the beams.

Beam	Steel	A_s	ρ	A'_s	ρ′	A_{sw1}	A_{sw2}
B01.ER.2f8.2f10.f6@180	ER	2f8	0.168	2f10	0.262	f6@180	f6@180
B02.NR.2f8.2f10.f6@180	NR	2f8	0.168	2f10	0.262	f6@180	f6@180
B03.ER.2f10.2f10.f6@180	ER	2f10	0.262	2f10	0.262	f6@180	f6@180
B04.NR.2f10.2f10.f6@180	NR	2f10	0.262	2f10	0.262	f6@180	f6@180
B05.ER.6f12.2f10	ER	6f12	1.132	2f10	0.262	f6@60	–
B06.NR.6f12.2f10	NR	6f12	1.132	2f10	0.262	f6@60	–
B07.ER.6f12.2f10.f6@60	ER	6f12	1.132	2f10	0.262	f6@60	f6@60
B08.NR.6f12.2f10.f6@60	NR	6f12	1.132	2f10	0.262	f6@60	f6@60
B09.ER.6f12.2f10.f6@180	ER	6f12	1.132	2f10	0.262	f6@60	f6@180
B10.NR.6f12.2f10.f6@180	NR	6f12	1.132	2f10	0.262	f6@60	f6@180
B11.NR.3f16.2f10AR0	NR	3f16	1.01	2f10	0.262	f6@60	–
B12.NR.3f16.2f10.f6@60AR0	NR	3f16	1.01	2f10	0.262	f6@60	f6@60
B13.NR.3f12.2f6.f6@60AR0	NR	3f12	1.01	2f6	0.095	f6@60	f6@60
B14.NR.3f16.3f16.f6@180AR0	NR	3f16	1.01	3f16	1.01	f6@180	f6@180
B15.NR.3f12.2f8.f6@60AR0	NR	3f12	0.565	2f8	0.168	f6@60	f6@60
B16.NR.3f12.2f8.f6@60	NR	3f12	0.565	2f8	0.168	f6@60	f6@60
B17.NR.3f12.2f8.f6@60AR0	NR	3f12	0.565	2f8	0.168	f6@60	f6@60
B18.NR.3f12.2f8.f6@180	NR	3f12	0.565	2f8	0.168	f6@180	f6@180
B19.NR.3f16.2f10.f6@180AR50	NR	3f16	1.01	2f10	0.262	f6@60	f6@180
B20.NR.3f16.2f16.f6@180AR50	NR	3f16	1.01	2f16	0.670	f6@60	f6@180
B21.NR.3f12.2f8.f6@180	NR	3f12	0.565	2f8	0.168	f6@60	f6@180
B22.NR.3f12.2f8.f6@60	NR	3f12	0.565	2f8	0.168	f6@60	f6@60
B23.NR.3f12.2f8.f6@60AR0	NR	3f12	0.565	2f8	0.168	f6@60	f6@60
B24.ER.2f6.2f6.f4@70	ER	2f6	0.38	2f6	0.38	f4@70	f4@70
B25.ER.3f6.2f6.f4@70	ER	3f6	0.57	2f6	0.38	f4@70	f4@70
B26.ER.4f6.2f6.f4@70	ER	4f6	0.75	2f6	0.38	f4@70	f4@70
B27.NR.3f8.2f6.f4@70	NR	3f8	1.01	2f6	0.38	f4@70	f4@70

The 27 beams were divided into 8 different groups. Although some beams from a given group may be related to beams from another group, the main distinction between groups lies in their construction and essential characteristics. The beams of Groups I, II, III, IV, and VI were built by the same company on the same day. Group I beams can be classified as almost insufficiently reinforced beams (ρ = 0.168%) (according to EC2, $\rho \geq 0.13\%$); beams in Group II are lightly reinforced beams (ρ = 0.262%); Group III beams are beams with a normal value of reinforcement ratio. The beams of Group IV were tested 1 year after their construction and the beams of Group VI were tested 2 years later, both subject to axial restraint. In the beams of Group V, it is possible to verify the effect of the axial restraint. The beams of Group VII, equivalent to the last 2 beams of Group V, were built at different times and tested by different people. There is emphasis on the superior (~20%) resistance of concrete to compression of beams in Group VII. The beams of Group VIII are of reduced dimensions (half the dimensions of the remaining beams).

With this extended set of beams, it is intended to show (unequivocally) the positioning of the cracks as well as the evolution of the crack widths throughout the development phase of the cracks. In addition, it is also important to analyze other aspects, such as the evolution of the cracking moment, or the cracking deflection, as a function of tensile reinforcement, or even the parameters that can influence the crack widths.

3.3. Materials

In the production of the beams, built in the laboratory, steel formwork was used. In the case of beams built externally (on a local company's site), a wooden formwork was used. The concretes were supplied by a ready-mixed concrete company, in different periods. In the case of beams of reduced dimensions, the mortar used was produced in the laboratory.

The values of the compressive strength f_c, relative to cubes with 150 mm of edge, were presented in Table 1.

Regarding the reinforcements, the strength characteristics of the tensioned steels used in each of the beam groups are presented in Table 3. ϕ indicates the diameter, f_y the yield strength of reinforcement, f_u the ultimate strength, and ε_u the strain of reinforcement at maximum load.

Table 3. Mechanical characteristics of reinforcement steel.

Group	Steel	ϕ	f_y (MPa)	f_u (MPa)	ε_u (%)
I	ER	8	585	631	4.74
	NR	8	532	635	14.5
II	ER	10	617	666	5.96
	NR	10	551	648	12.8
III	ER	12	604	653	6.14
IV	NR	12	541	632	13.7
VI	ER	16	552	647	4.8
	NR	16	575	684	13.6
V	NR	12	559	664	8.1
VII	NR	12	550	655	13.6
VIII	ER	6	577	828	6.49
	NR	8	634	726	11.1

4. Test Results

4.1. Crack Position

We start by mentioning that the title of this point is not "crack spacing". In fact, the cracks occur in the position of the stirrups. It does not mean that there will be cracks in all stirrup positions, nor does it mean that cracks between stirrups cannot occur. It means that the cracks, if they appear, occur first in the positions of the stirrups, if any.

In Figure 3, it is possible to visualize the positioning of the cracks in relation to the stirrups in the central zone (L_2) of Beams B01–B04. The failure of these beams occurred in the tensile reinforcement. Using the positioning of the LVDT (Linear Variable Differential Transformer) placed laterally to the beam (but in the center of the beam), it can be seen that the central crack is located about 5 mm to the left in the case of Beams B01 and B04; about 20 mm to the right in the case of Beam B02; and is centered on Beam B03. Two particularities to note: the line that identifies the position of the crack is drawn by hand slightly to the side (~10 mm) of the crack; remember that these beams were not produced in the laboratory, so any small deviations from the central stirrup must be assumed. Anyway, the remaining main cracks (two on each side) are located in the following stirrups, 180 mm spaced apart. Two important aspects should be highlighted: (i) the splitting of the cracks; (ii) the extra (secondary) cracks, arising between the main cracks of Beams B02 (2nd crack starting from the center to the right) and B03 (in the vertical direction of the right force point).

For Beams B05–B10, Figure 4 shows the cracks in the central zone (L_2). The failure of these beams occurred due to crushing of the compressed concrete and/or instability of the compressed reinforcement. Remember the absence of stirrups in central zone of Beams B05 and B06, a spacing of 60 mm apart between stirrups in Beams B07 and B08, and a spacing of 180 mm apart in Beams B09 and B10. For these beams, EC2 [1] determines a maximum spacing between cracks greater than 160 mm (80 mm minimum; average of 120 mm). Taking into account the number of spacings (10) between the main cracks of Beams B05 and B06 (beams without stirrups in central zone), and the value L_2 = 975 mm, the experimental (average) value of the spacing between cracks is less than 100 mm, i.e., much less than predicted (average) value.

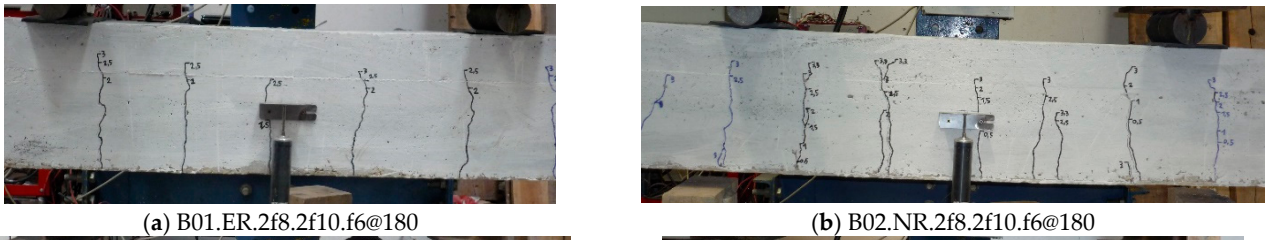

(**a**) B01.ER.2f8.2f10.f6@180 (**b**) B02.NR.2f8.2f10.f6@180

(**c**) B03.ER.2f10.2f10.f6@180 (**d**) B04.NR.2f10.2f10.f6@180

Figure 3. Crack position of Beams B01–B04.

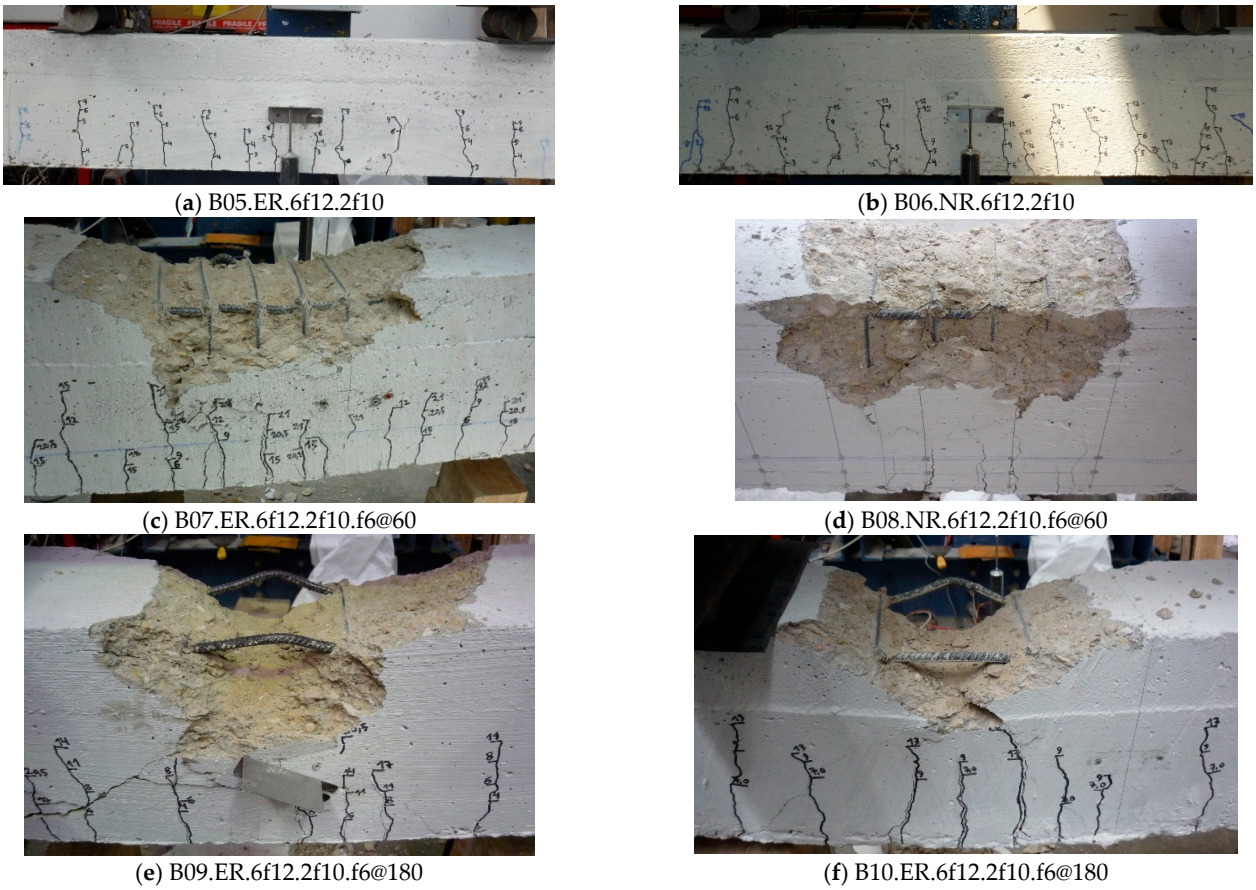

(**a**) B05.ER.6f12.2f10 (**b**) B06.NR.6f12.2f10

(**c**) B07.ER.6f12.2f10.f6@60 (**d**) B08.NR.6f12.2f10.f6@60

(**e**) B09.ER.6f12.2f10.f6@180 (**f**) B10.ER.6f12.2f10.f6@180

Figure 4. Crack position of Beams B05–B10.

If due attention had been paid at that time, it would have been very interesting to verify whether or not the first crack had occurred in the first stirrup of the lateral zones; in the first stirrup, the curvature is (a little) lower than the curvature in the central zone. In fact, these stirrups having (principal) cracks placed there, and thereafter an almost uniform spacing in the central zone; it is almost certain that this happened.

Figure 4c,d, relative to Beams B07 and B08 (stirrups spacing 60 mm apart), show that the cracks are preferentially positioned in the location of the stirrups. In the case of Beam B08, note the absence of the crack in the alignment of the 4th visible stirrup to the right. It is most likely that the crack has displaced too much (~30 mm) to the left.

Regarding Beams B09 and B10 (stirrups spacing 180 mm apart), Figure 4e,f show that the main cracks are positioned in the location of the stirrups. Secondary cracks form (posteriorly) between the main cracks.

A conclusion can already be drawn: cracking position does not depend on the type of reinforcement, whether of the ER type or of the NR type.

In Figure 5a, the cracks formed in Beam B11 are shown, which, as we recall, did not have any kind of transverse or compression reinforcement in the central zone. When the first cracks were detected, the locations of the first stirrups placed in the lateral zones had started cracking. In any case, an almost uniform distribution of formed cracks is visible, with an average spacing of around 100 mm (almost coinciding with the position of the demountable mechanical strain gauges DEMECs). This value is lower than the predicted average value (~120 mm). In Figure 5b,c, the stirrups are spaced 60 mm apart and the cracks are positioned according to the stirrups. In the case of Beam B13, there is no crack in the position of the first visible stirrup on the left. In Figure 5d, the stirrups are spaced 180 mm apart. It is possible to locate the cracks in the positions of the two visible stirrups. Among these, the secondary crack is in the middle.

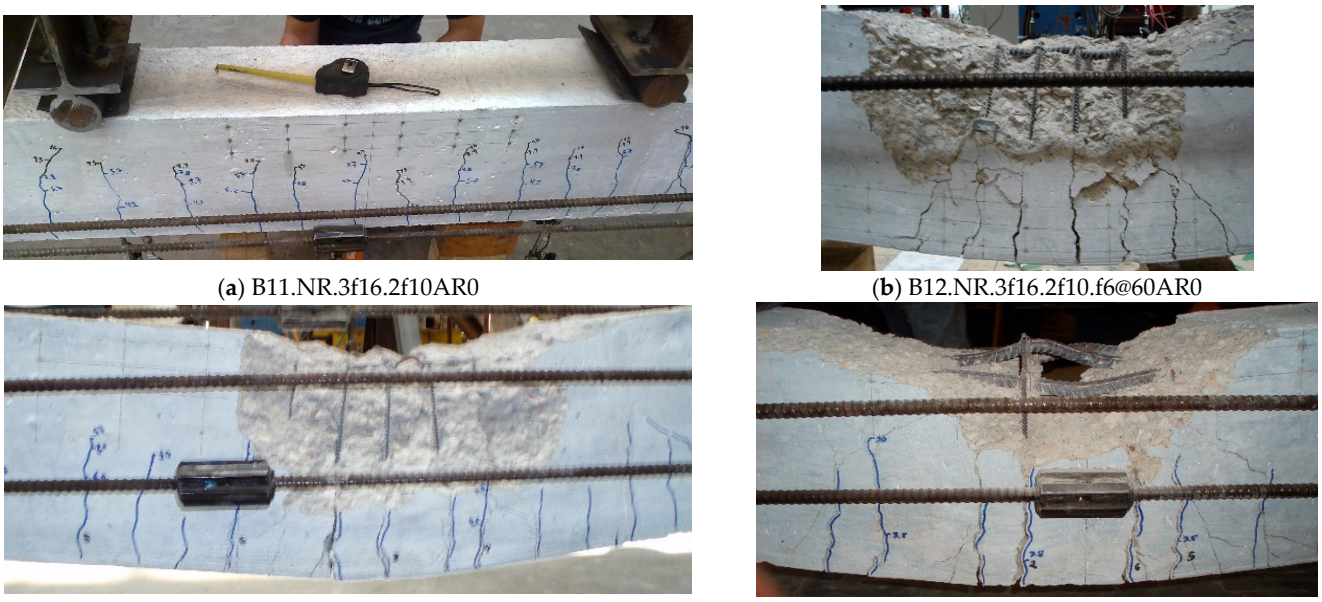

(**a**) B11.NR.3f16.2f10AR0 (**b**) B12.NR.3f16.2f10.f6@60AR0

(**c**) B13.NR.3f12.2f6.f6@60AR0 (**d**) B14.NR.3f16.3f16.f6@180AR0

Figure 5. Crack position of Beams B11–B14.

In Figure 6 are the images relating to Beams B15–B18. In Beam B15, it is possible to visualize the centerline of the beam—the only one placed among the DEMECs, 100 mm apart. In this line, there is no crack corresponding to the central stirrup. Three cracks on the left and two cracks on the right are located in the positions of the following stirrups, spaced 60 mm apart. In Beams B16 and B17, the coincidence of the cracks with the location of the stirrups is notorious. In Beam B18, with stirrups spaced 180 mm apart, the location of the central crack is visible, plus two main ones on each side. Among these are secondary cracks.

At the time of testing, Beams B19 and B20 were about 2 years old. Both with stirrups spacing 180 mm (in the center of the beam there is no stirrup), it is possible to confirm in Figure 7 that all stirrups (6) in the central zone had an associated (main) crack. The secondary cracks were positioned between these, with some irregularity.

Beams B21 and B22 were tested without active axial restraint. In the central zone, Beam B21 contains five stirrups spaced 180 mm apart. As before, in the position of the stirrups, the main cracks appeared and, among these, the secondary ones as well (Figure 8a). Beams B22 and B23 (Figure 8) have stirrups spacing 60 mm apart; there is a stirrup in the center of the beam. From the center of the beam, it is possible to verify the coincidence of the cracks

formed in relation to the positioning of the stirrups. On only Beam B23, just to the right of the central crack, two cracks are identified, instead of just one, close to the next stirrup.

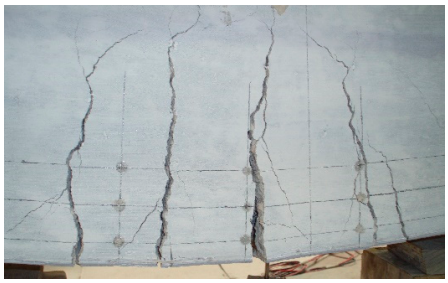

(**a**) B15.NR.3f12.2f8.f6@60AR0

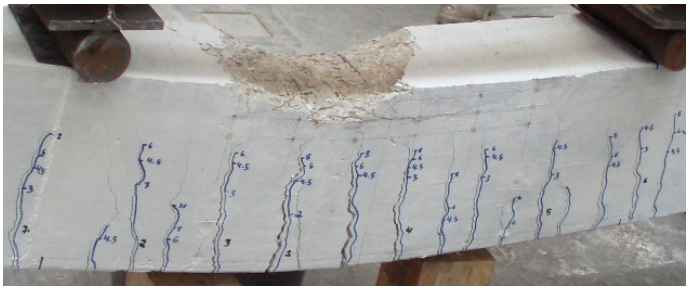

(**b**) B16.NR.3f12.2f8.f6@60

(**c**) B17.NR.3f12.2f8.f6@60AR0

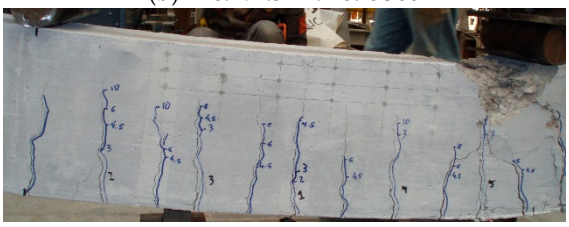

(**d**) B18.NR.3f12.2f8.f6@180

Figure 6. Crack position of Beams B15–B18.

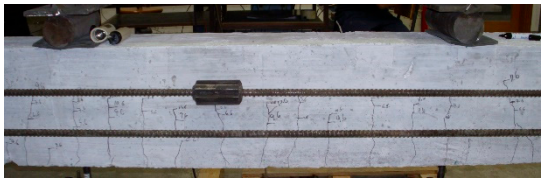

(**a**) B19.NR.3f16.2f10.f6@180AR50

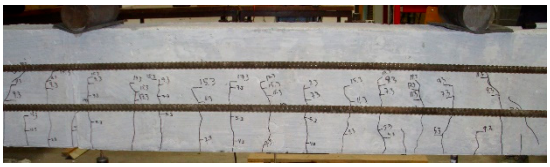

(**b**) B20.NR.3f16.2f16.f6@180AR50

Figure 7. Crack position of Beams B19–B20.

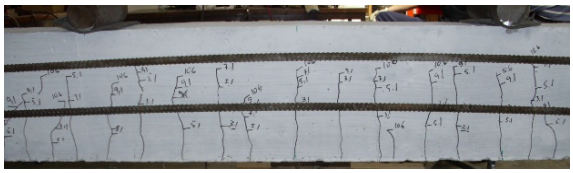

(**a**) B21.NR.3f12.2f8.f6@180

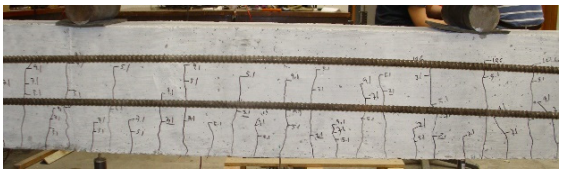

(**b**) B22.NR.3f12.2f8.f6@60

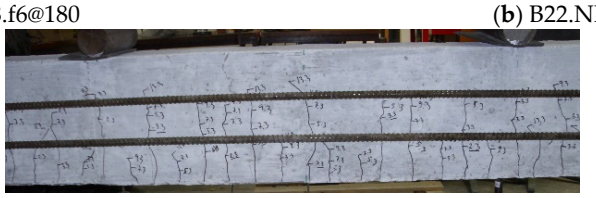

(**c**) B23.NR.3f12.2f8.f6@60AR0

Figure 8. Crack position of Beams B21–B23.

Figure 9 shows the positions of the cracks formed in the central zone of Beams B24–B26. Figure 9a shows the coincidence between the position of the cracks and the shear reinforcement. In Figure 9b,c, this coincidence is also almost complete for the seven stirrups in the central zone. It is important to note the double crack (instead of just 1) immediately to the right of the central crack. This double crack, which formed in Beams B25 and B26, results from the device used in the beams to ensure the cover (a small piece of steel ϕ10). The records relating to Beam B27 were lost on an SSD (solid-state drive) card. The authors ensure that the cracks were also located in the positions of the stirrups.

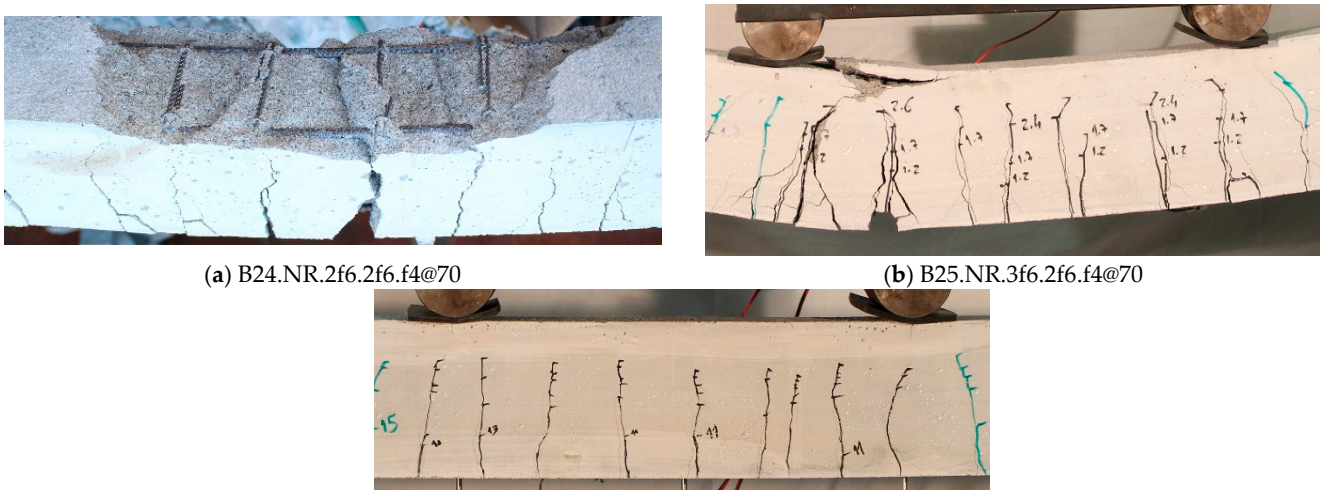

(**a**) B24.NR.2f6.2f6.f4@70 (**b**) B25.NR.3f6.2f6.f4@70

(**c**) B26.NR.4f6.2f6.f4@70

Figure 9. Crack position of Beams B24–B26.

In fact, this finding that the main cracks are formed preferentially in the position of the stirrups has been confirmed for a long time. In addition to these beams, the authors have already tested many others and have not been able to find any cases that suggest any other conclusion.

4.2. Cracking Moment

Several criteria can be established regarding the onset of cracking. In point 2.1, a possible criterion was presented, based on concrete strain. This criterion has generalized practical application in design and allows to know the cracking load. However, for a beam in a test, what is the cracking load? Better phrased: What is the cracking (concrete) strain? The visual criterion may be a more practical alternative. The authors can confirm that this visual criterion is not adequate. In fact, although it was possible to visualize (in some beams) crack widths of 0.01 mm, in fact, the cracking started with some previous load. This fact was (always) later confirmed in the P-d curves of the tests (P means total load and d the deflection).

The most suitable criteria are based on the P-d curve. One of the possibilities is to follow the following algorithm: (i) determine the line KI tangent to State I (elastic phase of the beam behavior) in the P-d diagram; (ii) determine the line KII tangent to State II (cracking development phase); (iii) determine the intersection point P_{int} between the lines KI and KII; (iv) the starting point of cracking is the point on the P-d curve closest to P_{int}; (v) the point, thus found on the P-d curve, determines the values of the cracking load P_{cr} and the cracking deflection d_{cr}.

For the various beams, Table 4 indicates the expected (mean) value of the tensile strength of the concrete f_{ct}, the expected (mean) value of the cracking moment M^*_{cr} (Equation (1)), the cracking load P_{cr}, the corresponding cracking moment M_{cr}, M^*_{cr}/M_{cr} quotient and the cracking deflection d_{cr}. For axially restrained beams, the value of the axial force at the cracking point N_{cr} is indicated.

In order to analyze the presented results, consider the following reduced cracking moment μ^*_{cr} defined by

$$\mu^*_{cr} = \frac{M_{cr}}{b.h^2.f_{ct}} \tag{4}$$

As the first hypothesis, Figure 10 shows the graph of reduced moments μ^*_{cr} evaluated for beams considered as a function of reinforcement ratio ρ. The cross markers represent Beams B19 and B20, where the axial force at the beginning of cracking was not insignificant (N_{cr} ~ 51 kN). The remaining beams are represented by circle markers. The indicated trend line was evaluated only for these beams. In this figure, the line corresponding to the

cracking moment determined by Equation (1) is also represented, assuming the proposal indicated in Structural Concrete [26], i.e., that f_{ct} is determined by concrete flexural tensile strength $f_{ctm,fl}$ (Equation (2)). Considering the value of R2 (determination coefficient), there is a significant dispersion of results for the different beams. This dispersion is more evident in tests with normally reinforced beams (ρ > 1%). Anyway, the trend line clearly shows the influence of tensioned reinforcement on cracking; the cracking moment in well-reinforced beams (ρ ~ 1.3%) reaches twice the value of insufficiently reinforced beams (ρ ~ 0.2%). Considering the value of the cracking moment estimated by Equation (1), it appears that, for weakly reinforced beams (ρ < 0.6%), the estimate is insecure, whereas the estimate is conservative for normally reinforced beams (ρ > 0.6%). This conclusion depends on the assumed value for f_{ct}.

Table 4. Beams strength at cracking point.

Beam	f_{ct} (MPa)	M^*_{cr} (kN.m)	P_{cr} (kN)	M_{cr} (kN.m)	M^*_{cr}/M_{cr}	d_{cr} (mm)	N_{cr} (kN)
B01	2.81	9.21	15.0	7.13	1.29	0.44	x
B02	2.81	9.21	16.3	7.76	1.19	1.137	x
B03	2.80	9.19	14.5	6.86	1.34	0.409	x
B04	2.81	8.71	16.1	7.66	1.14	0.496	x
B05	2.81	9.15	24.8	11.78	0.78	0.715	x
B06	2.83	8.43	26.1	12.38	0.68	0.836	x
B07	2.79	8.29	24.44	11.61	0.71	0.855	x
B08	2.78	8.61	22.34	10.61	0.81	0.809	x
B09	2.83	7.14	25.18	11.96	0.60	0.78	x
B10	2.77	8.59	33.46	15.89	0.54	1.027	x
B11	3.52	10.73	17.6	8.36	1.28	0.47	0.1
B12	3.52	10.90	15.3	7.27	1.50	0.831	0.5
B13	3.52	10.90	17.8	8.46	1.29	0.573	0.3
B14	3.51	11.15	25.6	12.16	0.92	0.652	0.45
B15	3.19	10.09	21	9.98	1.01	0.731	0.2
B16	3.18	9.77	19.6	9.31	1.05	0.767	x
B17	3.17	10.03	20.9	9.93	1.01	0.72	0.15
B18	3.18	9.73	20.7	9.83	0.99	0.798	x
B19	3.56	10.66	31.43	14.93	0.71	0.901	49.9
B20	3.56	10.66	34.41	16.34	0.65	1.029	52.2
B21	3.69	11.69	24.27	11.53	1.01	0.8	x
B22	3.69	11.51	21.49	10.21	1.13	0.606	x
B23	3.66	11.32	20.55	9.76	1.16	0.628	0.6
B24	4.49	1.70	6.44	1.53	1.11	0.42	x
B25	4.49	1.75	7.83	1.86	0.94	0.456	x
B26	4.50	1.78	8.32	1.98	0.90	0.609	x
B27	4.52	1.78	9.06	2.15	0.83	0.662	x

In order to assess the impact of the value assumed for f_{ct}, in Figure 11, (second hypothesis), the same values indicated in Figure 10 are presented, if the proposal of the CEB manual [25] ($f_{ct} = 0.7f_{ctm}$) were adopted, which coincides with Leonhardt's proposal [8]. It is only interesting to conclude that the cracking moment should not be evaluated following the suggestion of the CEB manual. Even the EC2 Handbook's [24] ($f_{ct} = f_{ctm}$) suggestion leads to extremely conservative results.

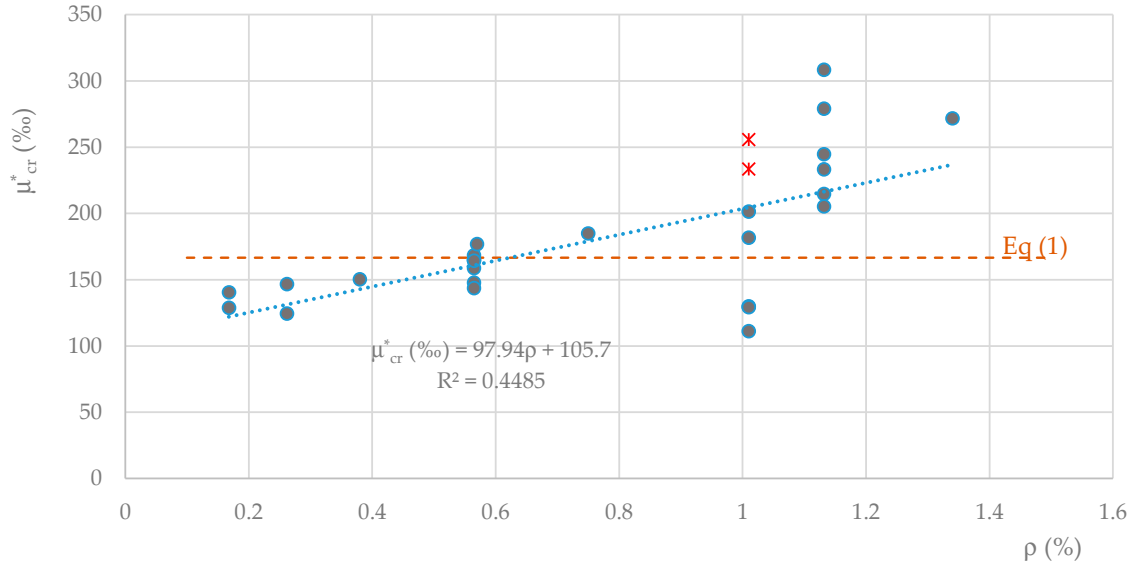

Figure 10. Cracking reduced moments. Hypothesis 1.

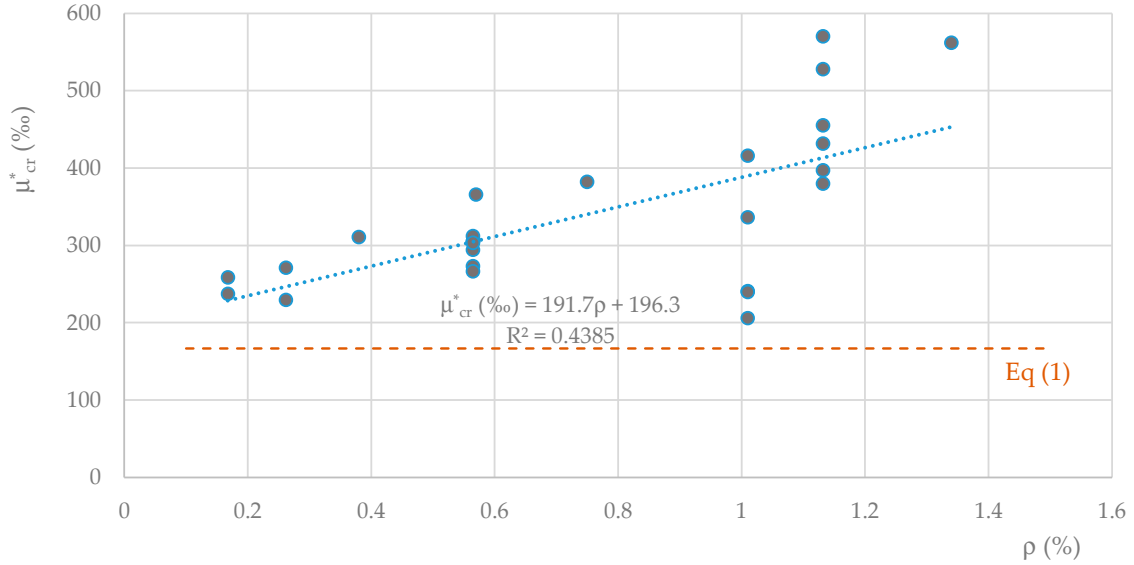

Figure 11. Cracking reduced moments. Hypothesis 2.

4.3. Cracking Deflection

Resorting to the theory of elasticity, and considering only the bending deformation, the (theoretical) value of the sag of the beam (deflection), at the cracking point d^*_{cr}, would be evaluated by

$$d^*_{cr} = \frac{M_{cr}}{E.I}\left[\frac{L2}{8}(4L1 + L2) + \frac{L1^2}{3}\right] \quad (5)$$

where E indicates the concrete modulus of elasticity and I is the moment of inertia of concrete cross section.

For the considered beams, it is presented in Figure 12 the values of the quotient $\delta_{cr} = L/d_{cr}$ as a function of the tensile reinforcement ratio ρ; $L = 2L_1 + L_2$ represents the free span of the beam. Remember that this coefficient δ_{cr} is recurrent in the regulations for checking deformation (Deflection control) within the scope of the serviceability limit states SLS. Once again, the results of Beams B19 and B20 are highlighted with asterisk marks. The trendline does not consider these values. The horizontal line represents the average of the theoretical values (4722; STDV = 497) determined from Equation (5). The average value of

the experimental results is 4227 with a standard deviation STDV = 1221. This dispersion of results is clearly evident in the reduced value of the determination coefficient R2. Only the trendline is illustrated because there is a high number of samples. In any case, there is a tendency for d_{cr} to increase (slightly) as the tensile reinforcement ratio increases. This result, although it cannot be definitively assumed, is curious, nonetheless. In fact, cracking starts when the tensioned concrete reaches the ultimate strain. Now, if there is a greater amount of tensile reinforcement, it motivates higher tensile forces, which will be balanced in the compressed part with greater strains and an inferior neutral axis, i.e., greater curvature of the cross section. That is, the upper sag of the beam. In the absence of a strong dependence, it can be stated that, as the amount of reinforcement increases, there is a slight increase in the cracking deflection.

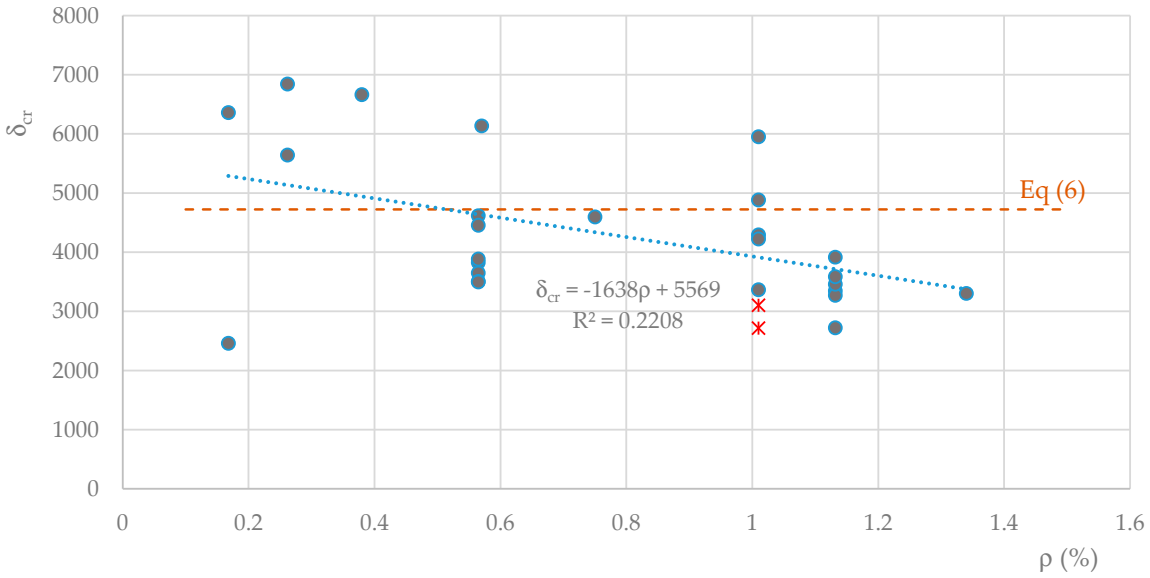

Figure 12. Cracking quotient $\delta_{cr} = L/d_{cr}$.

4.4. Cracking Width

Next, the graphs of the crack width values w. For the abscissa parameter, the deflection ratio d/L was chosen; d is the deflection of the beam. d/L can be referred to as reduced deflection. It is important to mention that this ratio, somehow, is (almost) directly proportional to the quotient L/h, but it is also proportional to the curvature and to the tensioned steel strain in central zone, where the first cracks arise and where the crack width was measured. Thus, the following graphs can be adapted for other beams, as long as the values of the abscissas are divided by the quotient L/h of these beams and multiplied by the new quotients.

The w-value results from the average of the three (if any) highest recorded values; in Beams B24–B27, the smallest, only two values were used. The crack widths were measured with the aid of a crack width microscope (40× magnification) at the level of the tensile reinforcement. For each beam, the first point represents the instant when it was possible to visualize the cracks. It was decided not to include, in these graphs, the starting point of cracking. The vertical lines represent the (supposed) yield point of the reinforcement. In these figures, it is important to understand the influence of the different parameters in terms of crack width in beams subjected to bending.

In Figure 13, the crack width w of the beams in Groups I (B01 and B02; $A_s = 2\phi 8$) and II (B03 and B04; $A_s = 2\phi 10$) are presented. The w-value varies "almost" linearly until the reinforcement yields. In these beams, whose failure occurred due to rupture of the tensile reinforcement, after yielding, there is a crack that opens for failure. The beams with a greater amount of reinforcement show smaller crack widths. In the beams of Group I, the visualization of cracking starts for values close to $d/L \approx 0.48‰$, with crack width

w ≈ 0.11 mm; in Group II, d/L ≈ 0.75‰ with w ≈ 0.07 mm. The beams of Group I yield approximately at a deflection ratio of d/L ≈ 2.84‰, with w ≈ 0.45 mm; in Group II, d/L ≈ 3.70‰ with w ≈ 0.35 mm. To conclude, regarding the type of steel (ER or NR), there are no differences to remark; only a slight reduction in w-value for beams with NR steel.

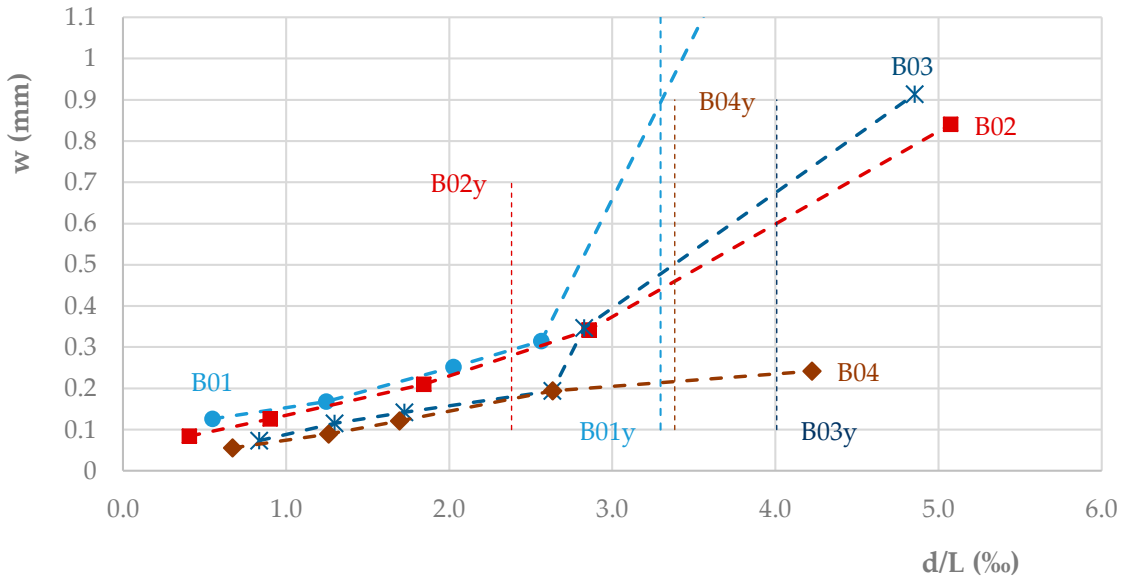

Figure 13. Cracking width. Beams in Groups I and II.

Figure 14 shows the crack width values for the beams in Group III. Regarding the type of steel, Beam B10, with NR steel, has higher w-values than Beam B09, the opposite of the previous. Therefore, the type of steel is not a relevant parameter for crack widths w. It is also possible to confirm the "almost" linearity in the variation of w until the reinforcement yields. Recall that Beams B05 and B06, without stirrups in the central zone L_2, are the ones with the lowest w-value. Beams B07 and B08, with stirrups spaced 60 mm apart, are the ones with the highest w-values, except for the case of Beam B10 close to yielding. Considering that the w-values in this graph are much lower than those in the previous graph, it is possible to confirm that, to the same reduced deflection, the crack widths decreases by increasing the tensile reinforcement. For these beams, cracking visualization started at a deflection ratio of d/L ≈ 0.67‰, with a crack width of w = 0.032 mm (which is much smaller than the previous values). In turn, yield occurred at a deflection ratio of d/L ≈ 5.2‰ (later), with a crack width of w ≈ 0.18 mm.

Figure 15 presents the crack width values for the beams in Group IV. These beams, with tensile reinforcement equivalent to those of Group III, were tested with axial restraint and were about 1 year old at the time of testing. As seen earlier, the effect of axial restraint on crack initiation is negligible (N_{cr} < 0.5 kN), but it becomes more significant as the beams approach yield (N_y(B11–B13) < 31 kN and N_y(B14) ≈ 54 kN). However, its impact is not such as to condition the conclusions in terms of deformations. The visualization of cracking started at a deflection ratio of d/L ≈ 1.1‰, with a crack width of w = 0.052 mm. These crack width values are higher than those determined for the beams in Group III. In turn, the yield occurred for equivalent amounts: d/L ≈ 5.2‰, with w ≈ 0.18 mm. These results suggest that the difference in age between the beams tested at one month and those tested at one year old did not significantly affect the evaluation of crack width.

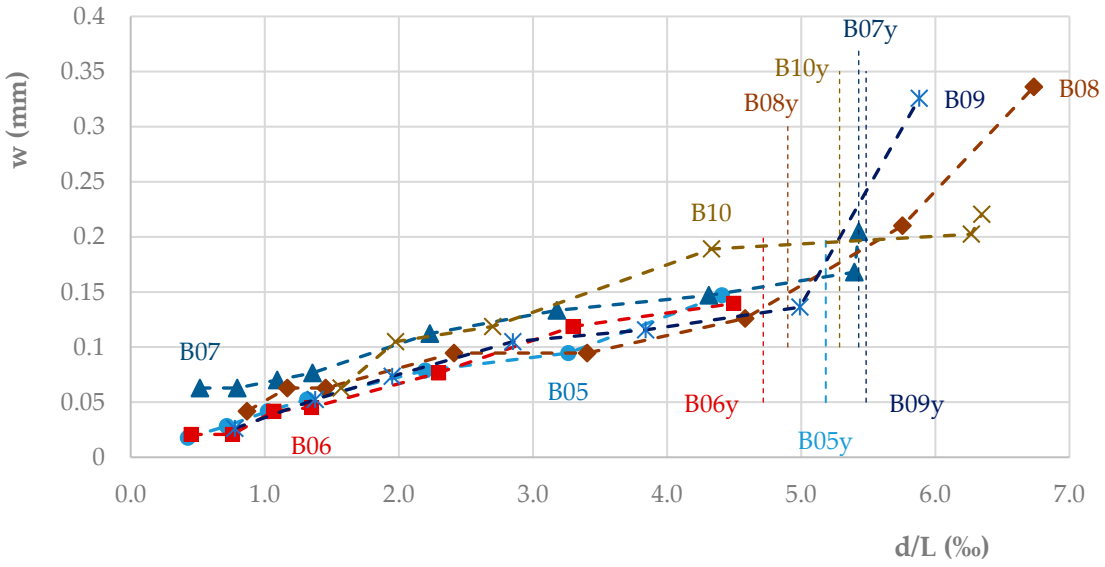

Figure 14. Cracking width. Beams in Group III.

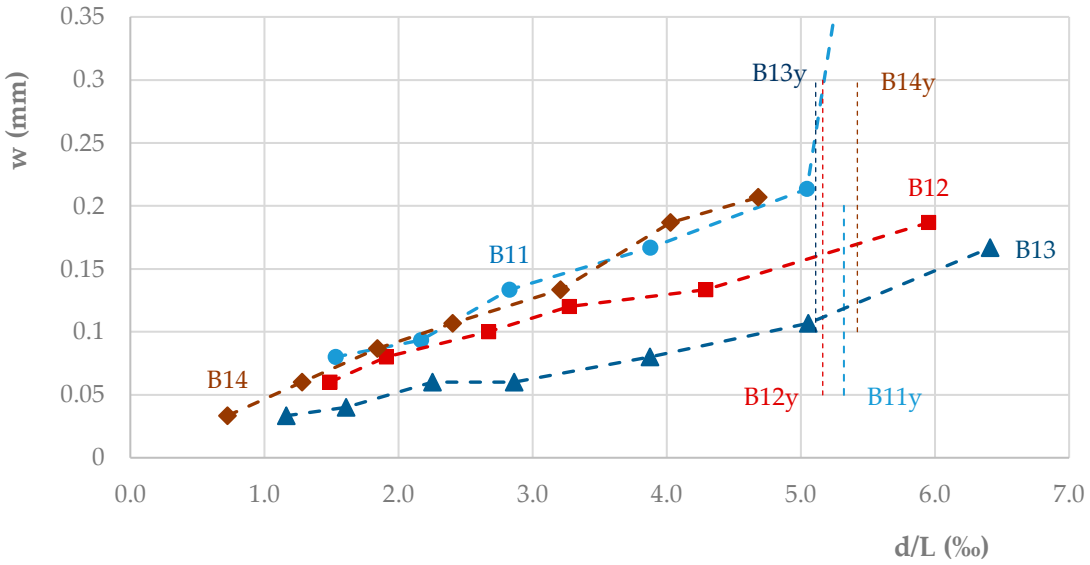

Figure 15. Cracking width. Beams in Group IV.

Most notable is the influence of the spacing of the stirrups. If the previous experiments with Group III beams suggest that crack width w tended to increase as the stirrup spacing s decreased, the opposite appears to be true for the beams in this group. Beams B11 (without stirrups in L_2 zone) and B14 (with a stirrup spacing of 180 mm) have higher crack width values, while Beams B12 and B13 (with a stirrup spacing of 60 mm) have significantly lower values. This highlights the difference between B12 (A's = 2ϕ10) and B13 (A's = 2ϕ6); Beam B13, which had a reduced amount of compression reinforcement, showed the lowest crack width values. That is, a greater amount of compressed reinforcement tends to increase the crack widths for the same sag. It is possible that the high crack width values observed in Beam B14 (A's = 3ϕ16; N_y(B14) ≈ 54 kN) were primarily due to the amount of compressed reinforcement.

Figure 16 shows the w-values for the beams in Group V, containing about half of the tensile reinforcement compared to the beams in the previous two groups. Two beams were tested with axial restraint: N_y(B15) = 33.7 kN and N_y(B17) = 29.7 kN. The first shows the highest values w; the second, the smallest. Therefore, the axial restraint is not a relevant parameter for crack width in terms of deflection ratio.

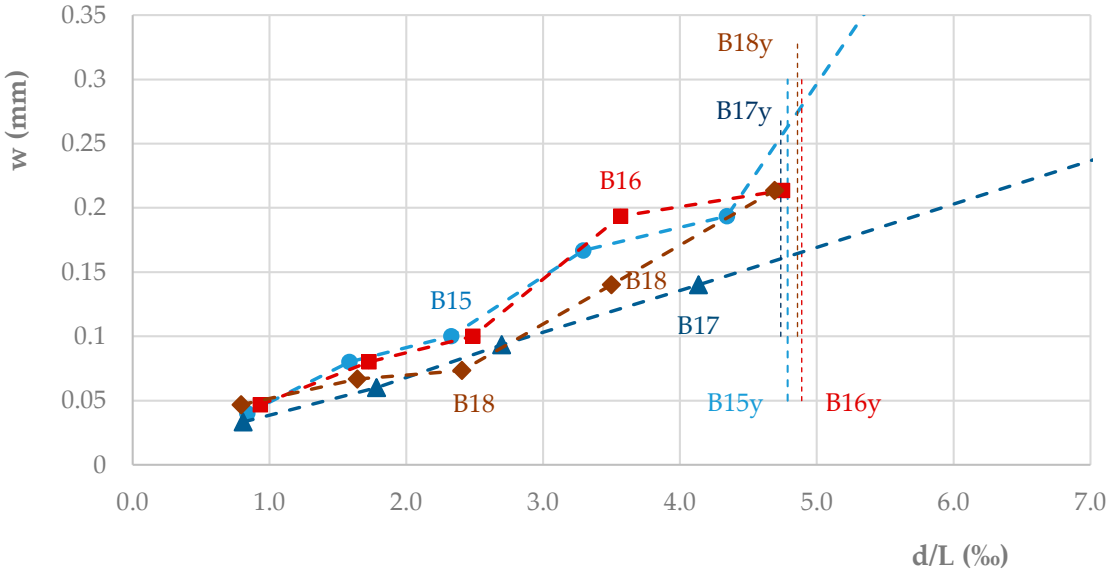

Figure 16. Cracking width. Beams in Group V.

Notably, in Group V, Beam B18 (s = 180 mm) shows smaller w relative to Beam B16 (s = 60 mm), which raises the question of whether a smaller spacing of the stirrups contributes to higher w-values in the short term, but in the long term, the opposite is observed. In any case, the visualization of cracking started at d/L ≈ 0.84‰, with w = 0.042 mm. These values are higher than those determined for the Group III beams. In turn, the yield occurred for equivalent amounts, with d/L ≈ 4.8‰ and w ≈ 0.2 mm. These values confirm that the lower tensile reinforcement there is, the greater the w-value and the sooner the yield occurs.

The w-values of the beams in Group VI (A_s = 3ϕ16) are shown in Figure 17. These beams were tested at about 2 years old. Here, the axial constraint was initially activated: N_{cr} ≈ 51 kN and N_y ≈ 120 kN. It is also important to point out that it was used a self-compacting concrete with shrinkage reducing admixtures. The lower w-values of Beam B19 (A's = 2ϕ10) relative to Beam B20 (A's = 2ϕ16) confirm that less compressive reinforcement results in lower w-values and later yielding. For these beams, cracking visualization started at d/L ≈ 0.67‰, with w = 0.020 mm. In turn, the yield occurred for equivalent amounts; d/L ≈ 4.9‰, with w ≈ 0.20 mm. Regarding the previous results (Groups III and IV), the comparison must consider the axial restriction. In any case, yield occurs for a similar sag, with a deviation of less than 6.5%; the w-value is relatively higher, with about 11% deviation.

In order to be able to compare with Beam B19, the curve related to Beam B12 was added to Figure 17. These beams are equivalent, differing only in that Beam B12 was tested at about 1 year old and with passive axial restraint: N_{cr} = 0.1 kN and N_y = 30.8 kN. In terms of shrinkage, due to the age of the beams, it is not believed that there are any impacts on the results. However, the axial constraint should have its effects, and it does, in terms of forces and moments. However, check the following: If one considers the beam subject to a compressive force of 120 kN, the resulting strain will be 66.7 μ (E_c = 30 GPa) in the concrete section (without steel). If one account for all this deformation for the crack widths, spaced 60 mm apart, it would be just 0.004 mm. This value is insignificant when compared with the maximum deviation of w-values between these two beams, which is about 0.03 mm. Therefore, the higher w-values of Beam B19, relative to Beam B12, close to yielding, can only result from the natural variability of experimental results.

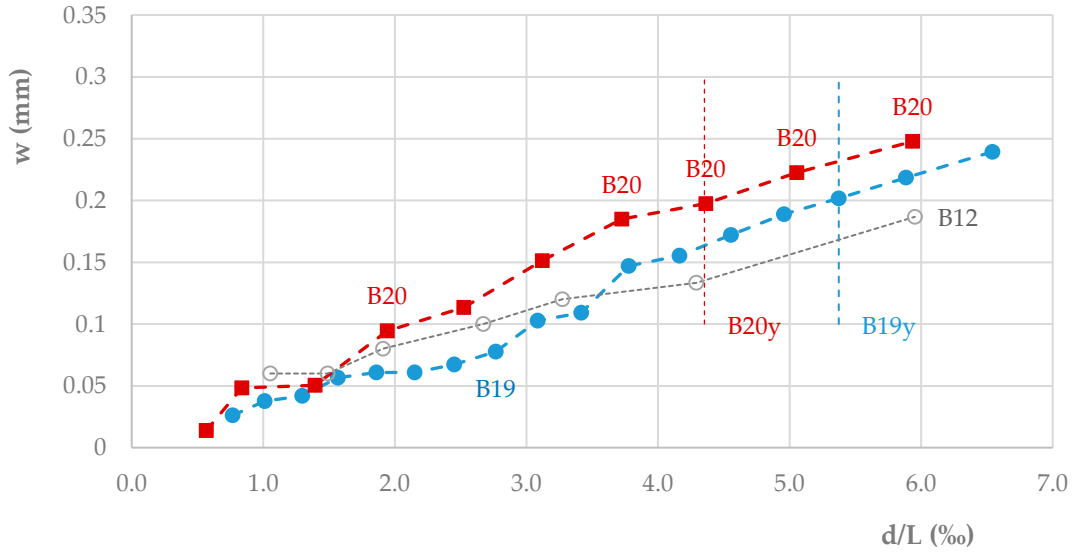

Figure 17. Cracking width. Beams in Group VI.

Figure 18 presents the w-values of the beams in Group VII (A_s = 3ϕ12). Only Beam B23 was subjected to passive axial restraint: N_{cr} = 0.6 kN and N_y = 60.0 kN. The visualization of cracking started at d/L ≈ 0.34‰, with w = 0.02 mm. In turn, the yield occurred for equivalent amounts: d/L ≈ 4.4‰, with w ≈ 0.21 mm. Regarding the beams of Groups III and IV (A_s = 3ϕ16), yielding occurs earlier (smaller deflection) and with higher w.

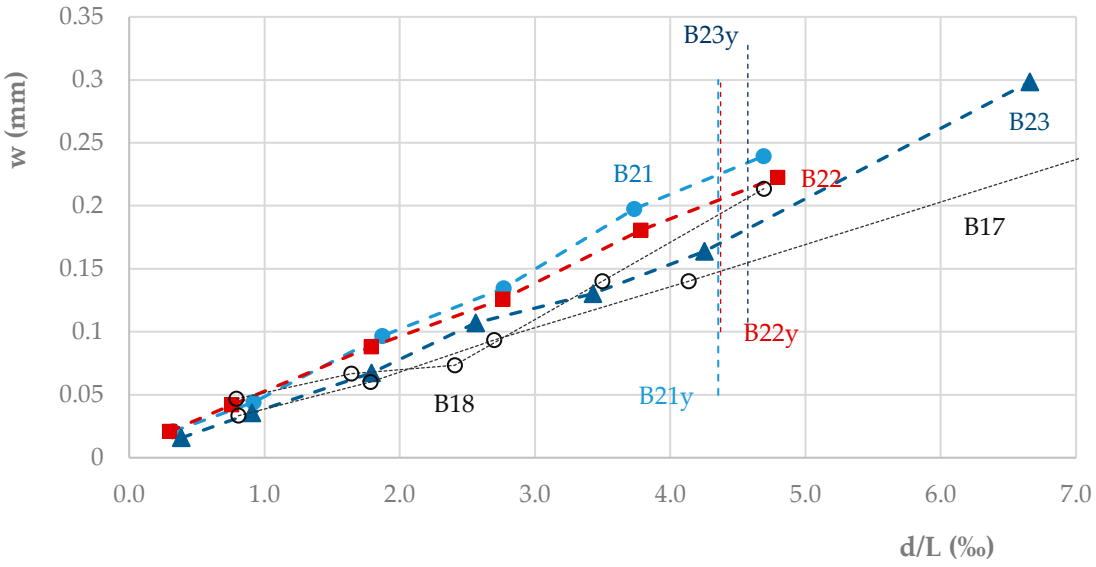

Figure 18. Cracking width. Beams in Group VII.

In Figure 18, the curves of Beams B17 (compare with Beams B22 and 23) and B18 (compare with Beam B21) were added. With the exception of one point, all w-deviations are less than 0.03 mm.

The w-values of the Group VIII beams are shown in Figure 19. These reduced dimensions beams have tensile reinforcement ratios varying between ρ = 0.38% and ρ = 1.01%. Considering the dimensions of these beams, relative to the previous ones, the measured loads are worth around 25%, the displacements around half, and the curvature is worth twice as much. However, the ratio d/L matches, as well as the w-value. This figure confirms the previous conclusions, namely, the reduction of w-value as the amount of tensile reinforcement increases. In any case, the w-values are somewhat lower than those determined in the previous beams.

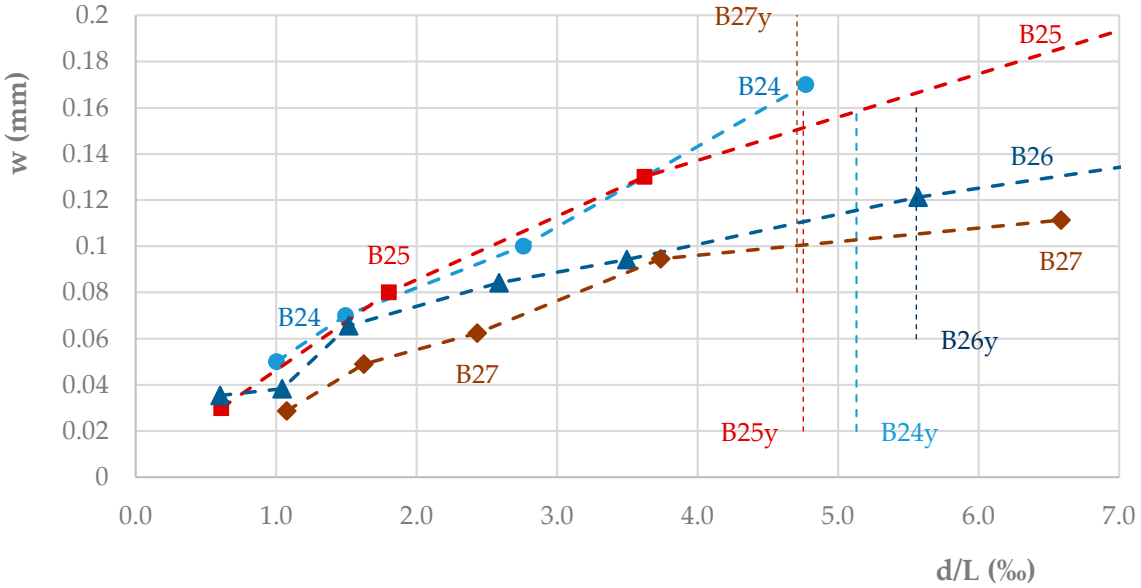

Figure 19. Cracking width. Beams in Group VIII.

5. Discussion

In this work, the authors revisit the issue of cracking in Civil Engineering structures. As it is known, cracking is a "necessary" phenomenon in RC elements, namely, in beams in order to take advantage of the potential of the reinforcement bars (strength). However, it is essential to find a way (controlling the crack widths) that prevents an unacceptable aesthetic of the structures and that might ensure a desired durability (protection of the reinforcement) throughout the working life of the structure. Although this topic has been extensively studied in the literature, the article focuses on aspects that have received limited attention in previous research.

The main objective of the authors was to show the location of the main cracks in reinforced concrete beams subjected to bending. The primary finding was that the cracks predominantly occur in the position of the shear reinforcements, contrary to the commonly known concept of "crack spacing". The study visually demonstrates that the location of the main cracks is closely linked to the positioning of the stirrups. The authors are aware of the avant-garde aspect of the results. In fact, these results will have influence on the usual computing procedures of crack width based on crack spacing. However, the authors reaffirm that this is the result of many years of experimental investigation, which are now unveiled. This article has been in preparation for a long period of time.

The study evaluated the cracking moment of reinforced concrete beams and determined that the mean flexural tensile strength of concrete should be used for this calculation. Neither the mean nor the characteristic value of axial tensile strength of concrete provided acceptable results for cracking moment evaluation. Additionally, the cracking moment was found to be strongly dependent on the tensile reinforcement ratio ρ, with a potential doubling of the cracking moment value for a 1.1% increase in the reinforcement ratio.

The study also revealed that the deflection at the onset of cracking increases slightly with an increase in the tensile reinforcement ratio ρ, with a 3% increase observed for every 0.1% increase in ρ.

An important conclusion drawn from this study is that crack width increases almost linearly with the sag/free span ratio during the development of cracks until yielding occurs. This relationship, which can be expressed in a dimensionless manner, depends on several key parameters, including (mainly) the tensile reinforcement ratio, the amount of compressed reinforcement, stirrup spacing, and axial confinement of the beam. This point is very important. If, in the specialized bibliography and in the codes of practice and standards, the crack width was calculated based on crack spacing (see Equation (1)),

and if this spacing is called into question in this work, then it is important to indicate an alternative way to carry out the calculation of the crack width.

The study suggests that increasing the tensile reinforcement ratio or providing axial confinement to the beam are effective methods for reducing crack widths. Conversely, increasing the amount of compressed reinforcement may result in wider cracks. As previously mentioned, for the same value of the deflection (that is, the same curvature), if the amount of reinforcement A_s increases, the horizontal balance of forces in the cross section is achieved with greater compression in the concrete (greater strains) and smaller strains in the tensioned steel—therefore, with a smaller crack width. On the contrary, for the same value of the deflection (same curvature), if the amount of reinforcement A'_s increases, the balance in the cross section is achieved with less compression in the concrete (lesser strains) and greater steel strains—therefore, with a larger crack width. In turn, if some axial confinement is guaranteed to the beam (compressive axial force), the average strains in the cross section decrease and consequently do the strains in the steel; therefore, a smaller crack width takes place. This effect is providentially achieved in bridges by applying prestressing.

The study found no evidence of the influence of concrete shrinkage or stirrup spacing on crack widths.

6. Conclusions

The main original conclusions of the work are presented:

1. The main cracks in RC beams, subject to bending, appear according to the positioning of the stirrups. This does not mean that primary cracks will be found in all stirrups, and it also does not mean that, between (very widely spaced) stirrups, primary cracks do not come up.
2. The evaluation of the cracking moment in RC beams, subjected to bending, must be carried out based on the flexural tensile strength of the concrete. This is a suggestion to be included in the regulations.
3. The crack width value is linearly proportional to the sag/free span ratio during the development of cracks until yielding. It is an alternative way to evaluate the crack width in RC beams, subject to bending.

Author Contributions: All authors were involved in all parts of the work. All authors have read and agreed to the published version of the manuscript.

Funding: This research was sponsored by FEDER funds through the program COMPETE—Programa Operacional Factores de Competitividade, and by national funds through FCT—Fundação para a Ciência e a Tecnologia, under the project UIDB/00285/2020.

Institutional Review Board Statement: Not applicable.

Informed Consent Statement: Not applicable.

Data Availability Statement: The data presented in this study are available on request from the corresponding author. Data evaluated in laboratory tests belong to the authors and to the University of Coimbra and are not publicly available.

Acknowledgments: The authors would like to express their gratitude to the students João Tiago Figueiredo Fernandes, António Manuel Duarte Miguéis, Bruno Filipe Duarte Abreu, Telmo Fernandes Ferreira, and Andreia Simões Gonçalves, who have also collaborated in this investigation.

Conflicts of Interest: The authors declare no conflict of interest.

References

1. *EN 1992-1-1:2004*; Eurocode 2: Design of Concrete Structures. General Rules and Rules for Buildings. Comite Europeen de Normalisation CEN: Bruxelles, Belgium, 2004.
2. *ACI 318-19*; Building Code Requirements for Structural Concrete and Commentary. American Concrete Institute: Singapore, 2019; ISBN 978-1-64195-056-5.

3. Watstein, D.; Parsons, D.E. Width and Spacing of Tensile Cracks in Axially Reinforced Concrete Cylinders. *J. Res. Natl. Bur. Stan.* **1943**, *31*, 1. [CrossRef]
4. Borges, J.F.; Lima, J.A. Crack and deformation similitude in reinforced concrete. *RILEM Bull.* **1960**, *7*, 79–90.
5. Beeby, A.W. *An Investigation of Cracking on the Side Faces of Beams*; Technical Report; Cement and Concrete Association: London, UK, 1971; Volume 42, p. 466.
6. Lima, J.A.; Monteiro, V. *Cracking and Deformability*; CEB International Commission on Structural Concrete, Specialized Course C8, Laboratório Nacional de Engenharia Civil: Lisbon, Portugal, 1973.
7. Bažant, Z.P.; Oh, B.H. Spacing of Cracks in Reinforced Concrete. *J. Struct. Eng.* **1983**, *109*, 2066–2085. [CrossRef]
8. Leonhardt, F. Cracks and Crack Control in Concrete Structures. *J. Prestress. Concr. Inst.* **1988**, *33*, 124–145. [CrossRef]
9. Braam, C.R. *Control of Crack Width in Deep Reinforced Concrete Beams*; Meinema: Delft, The Netherlands, 1990; Volume 35, pp. 1–106.
10. Venkateswarlu, B.; Gesund, H. Cracking and Bond Slip in Concrete Beams. *J. Struct. Eng.* **1972**, *98*, 2663–2885. [CrossRef]
11. Ratnamudigedara, P. *Crack Spacing, Crack Width and Tension Stiffening Effect in Reinforced Concrete Beams and One-Way Slabs*; Griffith University: Brisbane, Australia, 2003. [CrossRef]
12. Piyasena, R.; Loo, Y.-C.; Fragomeni, S. Factors Influencing Spacing and Width of Cracks in Reinforced Concrete; New Prediction Formulae. *Adv. Struct. Eng.* **2004**, *7*, 49–60. [CrossRef]
13. Naotunna, C.N.; Samarakoon, S.M.S.M.K.; Fosså, K.T. A New Crack Spacing Model for Reinforced Concrete Specimens with Multiple Bars Subjected to Axial Tension Using 3D Nonlinear FEM Simulations. *Struct. Concr.* **2021**, *22*, 3241–3254. [CrossRef]
14. Hong, S.; Ko, W.-J.; Park, S.-K. New Analytical Approach of Flexural Crack Width Estimation for Reinforced Concrete Beams. *Adv. Struct. Eng.* **2013**, *16*, 1763–1777. [CrossRef]
15. Zhang, D.; Rashid, K.; Wang, B.; Ueda, T. Experimental and Analytical Investigation of Crack Spacing and Width for Overlaid RC Beams at Elevated Temperatures. *J. Struct. Eng.* **2017**, *143*, 04017168. [CrossRef]
16. Yao, X.; Guan, J.; Zhang, L.; Xi, J.; Li, L. A Unified Formula for Calculation of Crack Width and Spacing in Reinforced Concrete Beams. *Int. J. Concr. Struct. Mater.* **2021**, *15*, 42. [CrossRef]
17. Ghalehnovi, M.; Karimipour, A.; de Brito, J.; Chaboki, H.R. Crack Width and Propagation in Recycled Coarse Aggregate Concrete Beams Reinforced with Steel Fibres. *Appl. Sci.* **2020**, *10*, 7587. [CrossRef]
18. Rossi, E.; Randl, N.; Mészöly, T.; Harsányi, P. Effect of TRC and F/TRC Strengthening on the Cracking Behaviour of RC Beams in Bending. *Materials* **2021**, *14*, 4863. [CrossRef] [PubMed]
19. De Maio, U.; Greco, F.; Leonetti, L.; Nevone Blasi, P.; Pranno, A. A Cohesive Fracture Model for Predicting Crack Spacing and Crack Width in Reinforced Concrete Structures. *Eng. Fail. Anal.* **2022**, *139*, 106452. [CrossRef]
20. Makhlouf, H.M.; Malhas, F.A. The effect of thick concrete cover on the maximum flexural crack width under service load. *ACI Struct. J.* **1996**, *93*, 257–265.
21. Fantilli, A.P.; Ferretti, D.; Iori, I.; Vallini, P. Flexural Deformability of Reinforced Concrete Beams. *J. Struct. Eng.* **1998**, *124*, 1041–1049. [CrossRef]
22. Naotunna, C.N.; Samarakoon, S.M.S.M.K.; Fosså, K.T. Experimental Investigation of Crack Width Variation along the Concrete Cover Depth in Reinforced Concrete Specimens with Ribbed Bars and Smooth Bars. *Case Stud. Constr. Mater.* **2021**, *15*, e00593. [CrossRef]
23. Lopes, A.V.; Lopes, S.M.R. Importance of a Rigorous Evaluation of the Cracking Moment in RC Beams and Slabs. *Comput. Concr.* **2012**, *9*, 275–291. [CrossRef]
24. Beeby, A.W.; Narayanan, R.S. Designers' Handbook to Eurocode 2. In *Eurocode Design Handbooks*; Telford, T., Ed.; American Society of Civil Engineers [Distributor]: London, UK; New York, NY, USA, 1995; ISBN 978-0-7277-1668-2.
25. CEB. *CEB Design Manual on Cracking and Deformations*; École Polytechnique Fédérale de Lausanne: Lausanne, Switzerland, 1985.
26. Structural Concrete. *1: Introduction, Design Process, Materials*; Bulletin/Fédération Internationale du Béton, International Federation for Structural Concrete (fib): Lausanne, Switzerland, 1999; ISBN 978-2-88394-041-3.
27. Fédération Internationale du Béton. *Model Code 2010. 1*; Bulletin/Fédération Internationale du Béton, International Federation for Structural Concrete (fib): Lausanne, Switzerland, 2010; ISBN 978-2-88394-095-6.
28. Ghali, A.; Favre, R.; Elbadry, M. *Concrete Structures: Stresses and Deformations*, 3rd ed.; Spon Press: London, UK; New York, NY, USA, 2002; ISBN 978-0-415-24721-4.
29. Bouhjiti, D.E.-M.; Demri, N.; Huguet-Aguilera, M.; Erlicher, S.; Baroth, J. Probabilistic Analysis of the Crack Spacing in Reinforced Concrete Members under Tensile Loads—Numerical Investigation of Size Effects. *Eur. J. Environ. Civ. Eng.* **2022**, *26*, 5545–5568. [CrossRef]
30. Neville, A.M. *Properties of Concrete*, 4th ed.; Longman: London, UK, 2000.